Journal of Applied Analysis and Computation
Volume 16, Number 6, December 2026, 3046–3070
Website:http://www.jaac-online.com
DOI:10.11948/20260019

ANALYSIS OF AN IMPULSIVE TUMOR-CHEMOTHERAPY MODEL WITH MICHAELIS-MENTEN NONLINEAR DRUG DEGRADATION

Changtong Li[1,†], Lifeng Wang[1], Xiaozhou Feng[1,†] and Yuntao Liu[2]

Abstract While chemotherapeutic drugs can rapidly debulk tumor populations, they also induce irreversible harm to healthy tissues. Therefore, precise control of both dosage and timing of administration is critical. In this study, we establish a class of tumor–chemotherapy models incorporating a nonlinear drug elimination rate, characterized by a Michaelis–Menten function. For the tumor-extinction subsystem, we employ blue principal branch of the Lambert W function to derive an analytical solution for the chemotherapy dose by solving the Michaelis-Menten equation, and construct an equivalent difference equation to establish the global stability of the fixed point. By combining the differential equation comparison theorem with Floquet multiplier analysis, we obtain explicit conditions for the local and global asymptotic stability of the tumor-free periodic solution and the permanence of the system. Additionally, using the bifurcation theorem, we establish explicit conditions for the existence of a stable positive periodic solution under the mechanism of system permanence. Numerical simulations further show that changes in the impulsive chemotherapy dose can drive a transition in the system dynamics, causing the tumor cells to evolve from a persistent state to an extinction state, thereby highlighting the decisive role of dose intensity in repeated chemotherapy. Moreover, small perturbations in the initial state can switch the long-term dynamics between tumor extinction and permanence, revealing bistability induced by the interaction between fixed-dose pulsed administration and nonlinear pharmacokinetics. Overall, this work provides a rigorous mathematical framework for analyzing dose–time effects in chemotherapy and offers valuable guidance for the design of clinical treatment regimens.

Keywords Chemotherapeutic drug, Michaelis-Menten function, Lambert W function, stability, permanence, bifurcation.

MSC(2010) 34A37, 34C23, 34D23, 92B05.

1. Introduction

Cancer remains one of the most serious threats to human health and continues to impose a substantial burden on public health systems worldwide. Recent statistics indicate that, in the United States alone, an estimated 2,001,140 new cancer cases and 611,720 cancer deaths are expected in 2024, highlighting the continuing importance of optimizing therapeutic strategies

[†]The corresponding author.
[1]Department of Mathematics, School of Science, Xi'an Technological University, No. 2, Xuefu Middle Road, Weiyang District, Shannxi Province, Xi'an 710032, China
[2]Department of Statistics, School of Mathematics, Southwest Jiaotong University, Sichuan Province, Chengdu, China
Email: lichangtong@xatu.edu.cn(C. Li), 18291534060@163.com(L. Wang), fengxz@xatu.edu.cn(X. Feng), liyto22@my.swjtu.edu.cn(Y. Liu)

in oncology [25, 30]. Among the available treatment modalities, chemotherapy remains a fundamental approach for suppressing tumor progression, reducing tumor burden, and supporting combination therapy. However, the efficacy of chemotherapy is not determined solely by the administered dose itself. It also depends strongly on the dosing interval, the permanence of drug exposure in vivo, and the tolerance of normal tissues. Excessive treatment intensity may induce severe toxicity, whereas insufficient dosing or poorly scheduled administration may weaken tumor suppression and even promote relapse or therapeutic resistance. Therefore, clarifying the coupled relationship among dose, timing, and treatment outcome from a dynamical perspective is of both theoretical and practical importance [4, 13].

The development of mathematical oncology has provided a systematic framework for understanding tumor evolution and designing therapeutic strategies. Early studies on tumor–immune interactions showed that even relatively simple nonlinear systems may exhibit rich dynamical behaviors such as permanence, dormancy, bistability, and bifurcation, among which the work of Kuznetsov et al. is widely regarded as a foundational contribution to quantitative tumor–immune modeling [11, 27]. Subsequently, de Pillis et al. developed a classical chemo-immunotherapy model that revealed therapeutic synergy and provided biological interpretations of combined treatment effects [6, 22]. Building on these developments, increasing attention has been paid to treatment scheduling, combination therapy, and optimization, demonstrating that mathematical models can support both mechanistic understanding and quantitative design of treatment regimens [1, 19, 24].

Despite these advances, two major issues remain in current mathematical models of chemotherapy. First, many tumor–drug models idealize chemotherapy administration as a continuous input process, whereas in clinical practice chemotherapeutic agents are usually delivered at discrete times or within short dosing windows, followed by intervals during which drug metabolism and tumor evolution proceed continuously. Thus, the real treatment process is intrinsically characterized by the coexistence of instantaneous intervention and continuous evolution. Previous studies have shown that impulsive differential equations are more suitable than continuous-input models for representing fixed-time dosing, different treatment frequencies, and scheduling mismatch [7, 20, 37]. Second, many existing models still adopt a linear drug elimination law to describe the decay of chemotherapeutic agents in vivo. From a pharmacokinetic perspective, however, when drug metabolism is affected by enzymatic saturation and related nonlinear mechanisms, the clearance rate is no longer proportional to drug concentration, and Michaelis–Menten-type kinetics offers a more realistic description [5, 9, 23, 29]. More recently, Pierik et al. further showed that higher-order nonlinear effects in chemotherapy pharmacodynamics and pharmacokinetics may significantly influence tumor regression and cachexia, underscoring the importance of incorporating more realistic PK/PD nonlinearities into mathematical models [21, 31, 34, 36]. In parallel, recent studies on infectious-disease dynamics have highlighted the growing importance of advanced stochastic and intelligent modeling frameworks for capturing biological complexity, uncertainty, and intervention effects, such as within-host chikungunya virus transmission with latency and vaccination-mediated COVID-19 control [8, 16, 32]. These developments, although arising from a different biomedical context, further demonstrate that integrating nonlinear mechanisms, temporal heterogeneity, and data-informed computational strategies is essential for improving the realism and predictive capability of mathematical models of treatment dynamics.

Recent studies have further advanced this direction. Tang et al. analyzed synergistic and dose-dependent effects in combined radio- or chemotherapy with immunotherapy [28]; Yosef and Bunimovich-Mendrazitsky developed a more treatment-specific mathematical model for MMC

chemotherapy in bladder cancer [35]; and Liliopoulos et al. compared periodic and intermittent chemotherapy schedules from an optimal-control perspective, emphasizing the importance of dosing design in tumor suppression [17].

Motivated by the above considerations, this paper investigates an impulsive tumor–chemotherapy model with fixed-time administration and Michaelis–Menten nonlinear drug elimination

$$\begin{cases} \left.\begin{aligned} H'(t) &= rH(t)(1-\eta H(t)) - \frac{\alpha H(t)}{1+\omega H(t)} - kD(t)H(t) \\ D'(t) &= -\frac{\beta D(t)}{K+D(t)} \end{aligned}\right\} t \neq n\tau, \\ \left.\begin{aligned} H(t^+) &= H(t) \\ D(t^+) &= D(t) + \tilde{\sigma} \end{aligned}\right\} t = n\tau, \end{cases} \tag{1.2}$$

where $H(t)$ denotes the density of tumor cells at time t, and $D(t)$ denotes the concentration of the chemotherapeutic drug at time t. The parameter r is the intrinsic growth rate of tumor cells, and $\frac{1}{\eta}$ represents the environmental carrying capacity for the tumor population. The term $\frac{\alpha H(t)}{1+\omega H(t)}$ is a Holling type II functional response describing the baseline inhibitory effect of the host immune system on tumor cells, where α denotes the maximum immune-induced inhibition rate and ω characterizes the saturation effect of the immune response. The term $kD(t)H(t)$ represents the killing effect of the chemotherapeutic drug on tumor cells, where k is the drug-induced tumor cell killing coefficient. The drug elimination process is governed by the Michaelis–Menten term $\frac{\beta D(t)}{K+D(t)}$, where β denotes the maximum elimination rate of the drug and K is the Michaelis–Menten constant, namely, the half-saturation constant of drug degradation. The parameter τ denotes the treatment period, and $\tilde{\sigma}$ is the dose of the chemotherapeutic drug administered at each impulsive treatment time $t = n\tau$ ($n \in \mathbb{N}_+$). Here, $H(t^+)$ and $D(t^+)$ denote the right-hand limits of $H(t)$ and $D(t)$ immediately after impulsive administration, respectively. Unless otherwise stated, all parameters are assumed to be positive. In addition, the initial conditions are taken as $H(0) = H_0 > 0$ and $D(0) = D_0 \geq 0$, where H_0 and D_0 denote the initial tumor cell density and the initial drug concentration, respectively.

In contrast to many existing models built upon continuous administration or linear elimination assumptions, the present study does not seek to construct a highly complex multivariable clinical prediction framework. Instead, we propose a two-dimensional impulsive dynamical system that retains both biological interpretability and mathematical tractability, with the aim of characterizing the coupled influence of periodic dosing and nonlinear drug elimination on the long-term evolution of the tumor. In particular, we focus on the interplay among the impulsive dose, treatment period, and maximal drug elimination capacity, and on how these factors jointly determine whether the tumor persists or is ultimately eradicated.

The main contributions of this work are summarized as follows. First, we establish a tumor–chemotherapy model incorporating fixed-time impulsive drug administration and Michaelis Menten nonlinear drug elimination, and we explicitly define the biological meanings of all variables and parameters. Second, we analyze the positivity, boundedness, and existence of solutions, thereby providing the theoretical basis for the subsequent study of stability and the existence of positive periodic solutions. Third, by examining the coupled dynamical relationship between the drug subsystem and the tumor subsystem, we derive threshold-type criteria that distinguish tumor permanence from tumor eradication. Finally, numerical simulations are performed to validate the theoretical findings and to systematically illustrate the effects of the impulsive

dose, treatment period, and nonlinear elimination parameters on the system dynamics and their biological implications.

The remainder of this paper is organized as follows. Section 2 presents the preliminaries and basic properties of the system. Section 3 discusses the existence of solutions and the corresponding conditions. Section 4 investigates the local and global stability of the tumor-extinction periodic solution. Section 5 is devoted to the existence of positive periodic solutions. Section 6 demonstrates, through numerical simulations, the effects of key parameters on the dynamical behavior of the system. Finally, Section 7 concludes the paper with a summary of the main results, together with a discussion of the model limitations and possible directions for future research.

2. Preliminaries

This section, we would like to introduce some concepts and definitions related to our system (1.2).

Definition 2.1. [2,9] The Lambert W function is characterized as a multi-valued inverse of the function $x \to x\exp\{x\}$, where it acts as a solution that satisfies

$$\text{Lambert } W(x)\exp\left\{\text{Lambert } W(x)\right\} = x.$$

Based on the definition above, the derivative of the Lambert $W(x)$ function can be expressed

$$\text{Lambert } W'(x) = \frac{\text{Lambert } W(x)}{x(1+\text{Lambert } W(x))},$$
$$\text{Lambert } W''(x) = \frac{\text{Lambert } W(x)^2 + \text{Lambert } W(x) + 1}{x^2(1+\text{Lambert } W(x))^3}.$$

Note that Lambert $W''(x) > 0$ always holds on the upper branch of Lambert W. Integral representations of Lambert W [3]

$$\int \text{Lambert } W(x)dx = x\left(\text{Lambert } W(x) - 1 + \frac{1}{\text{Lambert } W(x)}\right),$$

prove particularly useful for asymptotic analysis, as demonstrated in Figure 1.

Definition 2.2. The system(1.2) is termed a permanent system if there exist positive constants m and M. For all solutions $(H(t), D(t))$ with initial values $H(0) > 0, D(0) > 0$, it is required that $m < H(t) < M$ and $m < D(t) < M$ for all $t > \tau_0$. Notably, the value of τ_0 is not contingent on the initial conditions.

The following lemma will be used in proofs of our main results.

Lemma 2.1. [15,18] *Suppose $H(t)$ is a solution of system (1.2) with $H(0^+) \geq 0$, then $H(t) \geq 0$ for all $t \geq 0$. Also $D(t) \geq 0$, $t \geq 0$ if $D(0^+) \geq 0$.*

3. Global stability analysis of the model

3.1. The positivity and boundedness of system (1.2) solutions

Theorem 3.1. *Suppose $(H(t), D(t))$ is a solution of system (1.2) with $H(0^+) > 0$ and $D(0^+) > 0$, then $H(t) > 0$, $D(t) > 0$ for all $t > 0$.*

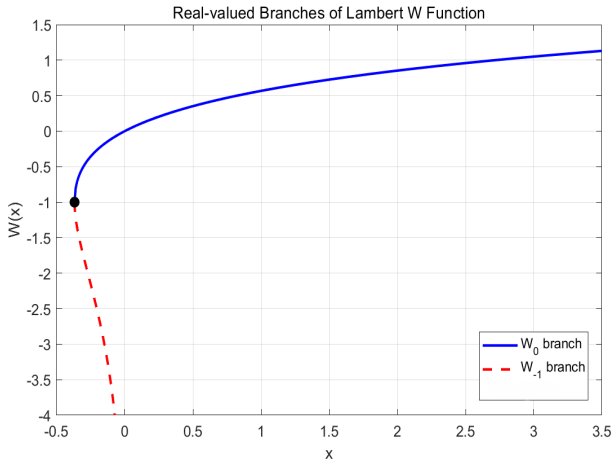

Figure 1. The Lambert W function $W(x)$ has two branch $W_0 : [\exp\{-1\}, \infty] \to [-1, \infty]$ and $W_{-1} : [\exp\{-1\}, \infty] \to [\infty, -1]$.

Proof. If exists $H(t) < 0$, then there exists t_0 such that $H(t_0) = 0$ and $H'(t_0) < 0$. However,

$$\lim_{t \to t_0} \frac{dH(t)}{dt} = rH(t_0)(1 - \eta H(t_0)) - \frac{\alpha H(t_0)}{1 + \omega H(t_0)} - kD(t_0)H(t_0) = 0,$$

which is a contradiction. Thus $H(t) > 0$ with $t > 0$. If $D(t) \leq 0$, then there must exists t_1 such that $D(t_1) = 0$ and $D'(t_1) < 0$. However

$$\lim_{t \to t_1} \frac{dD(t)}{dt} = -\frac{\beta D(t_1)}{K + D(t_1)}.$$

This constitutes a contradiction, implying that $D(t) > 0$ for $t > 0$. Consequently, since $(H(t), D(t))$ is positive for $H(0) > 0, D(0) > 0$ with $t > 0$. □

Next, we prove the boundedness of the system (1.2).

Theorem 3.2. *There exists a constant $M_0 > 0$ such that $H(t) \leq M_0$ for all t, where $H(t)$ is any solution of system (1.2) with all t.*

Proof. From the first equation of system (1.2), we obtain

$$\begin{aligned} \frac{dH(t)}{dt} &= rH(t)\big(1 - \eta H(t)\big) - \frac{\alpha H(t)}{1 + \omega H(t)} - kH(t)D(t) \\ &\leq rH(t) - r\eta H^2(t) \\ &= rH(t)\left(1 - \eta H(t)\right). \end{aligned}$$

By using the comparison principleon the interval $t \in (n\tau, (n+1)\tau]$, we have

$$H(t) \leq \max\left\{H(0), \frac{1}{\eta}\right\} = M_0.$$

Furthermore

$$\lim_{t \to \infty} \sup H(t) \leq M_0.$$

The boundedness of $D(t)$ will be rigorously established in subsequent analyses. □

3.2. Global stability of the tumor free periodic solution

Assume that during the entire treatment process, the number of tumor cells continuously decreases and eventually leads to the extinction of tumor cells. The corresponding chemotherapeutic agent subsystem is (3.1)

$$\begin{cases} D'(t) = -\dfrac{\beta D(t)}{K + D(t)}, t \neq n\tau, \\ D(t^+) = D(t) + \tilde{\sigma}, \quad t = n\tau. \end{cases} \tag{3.1}$$

Theorem 3.3. *Under the condition* $\frac{\tilde{\sigma}}{\tau} < \beta$ *for* $t \in (n\tau, (n+1)\tau]$ *and* $n \in Z_+$, *system* (3.1) *admits a globally asymptotically stable positive periodic solution given by*

$$\tilde{D}(t) = K \, Lambert \, W\left\{\frac{D^*}{K}\exp\left\{\frac{D^*}{K} - \frac{\beta}{K}(t - n\tau)\right\}\right\},$$

where $D^* = \frac{\tilde{\sigma}}{1-\exp\left\{\frac{1}{K}(\tilde{\sigma}-\beta\tau)\right\}}$.

Proof. From the first equation of system (3.1), we have

$$-\frac{K + D(t)}{\beta D(t)} dD(t) = dt,$$

from which direct integration yields

$$\ln\frac{D(t)}{D(n\tau^+)} + \frac{1}{K}\big(D(t) - D(n\tau^+)\big) = -\frac{\beta}{K}(t - n\tau).$$

Taking the exponential of both sides gives

$$\frac{D(t)}{D(n\tau^+)}\frac{\exp\left\{\frac{D(t)}{K}\right\}}{\exp\left\{\frac{D(n\tau^+)}{K}\right\}} = \exp\left\{-\frac{\beta}{K}(t - n\tau)\right\},$$

which holds for $t \in (n\tau, (n+1)\tau]$. Rearranging terms leads to

$$\frac{D(t)}{K}\exp\left\{\frac{D(t)}{K}\right\} = \frac{D(n\tau^+)}{K}\exp\left\{\frac{D(n\tau^+)}{K} - \frac{\beta}{K}(t - n\tau)\right\}. \tag{3.2}$$

By Definition 2.1, $D(t)$ remains strictly positive and continuous. Its analytical expression can be obtained using the principal branch(W_0) of the Lambert W function [2]. Specifically, $D(t)$ on the interval $t \in (n\tau, (n+1)\tau]$ is given by

$$D(t) = K \, \text{Lambert } W\left(\frac{D(n\tau^+)}{K}\exp\left\{\frac{D(n\tau^+)}{K} - \frac{\beta}{K}(t - n\tau)\right\}\right). \tag{3.3}$$

At the impulse moment $t = (n+1)\tau$, since

$$D(n\tau^+) = D(n\tau) + \tilde{\sigma},$$

it follows that

$$D((n+1)\tau^+) = K \, \text{Lambert } W\left\{\frac{D(n\tau^+)}{K}\exp\left(\frac{D(n\tau^+)}{K} - \frac{\beta\tau}{K}\right)\right\} + \tilde{\sigma}. \tag{3.4}$$

Using properties of the Lambert W function [29], equation (3.4) can be rewritten as

$$D((n+1)\tau^+) - \tilde{\sigma} = K \text{ Lambert } W\left\{\frac{D(n\tau^+)}{K}\exp\left(\frac{D(n\tau^+)}{K} - \frac{\beta\tau}{K}\right)\right\}. \tag{3.5}$$

Rearranging the above expression yields the following identity

$$\left(\frac{D((n+1)\tau^+)}{K} - \frac{\tilde{\sigma}}{K}\right)\exp\left\{\frac{D((n+1)\tau^+)}{K} - \frac{\tilde{\sigma}}{K}\right\} = \frac{D(n\tau^+)}{K}\exp\left\{\frac{D(n\tau^+)}{K} - \frac{\beta\tau}{K}\right\}.$$

Letting $D((n+1)\tau^+) = D_{n+1}$ and $D(n\tau^+) = D_n$, we obtain the difference equation

$$\left(\frac{D_{n+1}}{K} - \frac{\tilde{\sigma}}{K}\right)\exp\left\{\frac{D_{n+1}}{K} - \frac{\tilde{\sigma}}{K}\right\} = \frac{D_n}{K}\exp\left\{\frac{D_n}{K} - \frac{\beta\tau}{K}\right\}, \tag{3.6}$$

which is equivalent to

$$\frac{\frac{D_{n+1}}{K} - \frac{\tilde{\sigma}}{K}}{\frac{D_n}{K}} = \frac{\exp\left\{\frac{D_n}{K} - \frac{\beta\tau}{K}\right\}}{\exp\left\{\frac{D_{n+1}}{K} - \frac{\tilde{\sigma}}{K}\right\}}.$$

Therefore, difference equation (3.6) has a unique fixed point, denoted as D^*, which satisfies

$$D^* = D(n\tau^+) = D(0^+) = \frac{\tilde{\sigma}}{1 - \exp\left\{\frac{1}{K}(\tilde{\sigma} - \beta\tau)\right\}}. \tag{3.7}$$

Note that the concentration of the chemotherapeutic agent cannot be negative, therefore, the fixed point must satisfy the following conditions

$$\frac{\tilde{\sigma}}{\tau} < \beta,$$

when $t \in (n\tau, (n+1)\tau], n \in Z_+$.

The principal branch(W_0) of the Lambert W function yields a positive periodic solution (1.2)

$$\tilde{D}(t) = K \text{ Lambert } W\left\{\frac{D^*}{K}\exp\left\{\frac{D^*}{K} - \frac{\beta}{K}(t - n\tau)\right\}\right\}. \tag{3.8}$$

We now use the approach described in [15] to analyze the stability of positive periodic solution. Corresponding to difference equation (3.4), we define

$$F(D) = K \text{ Lambert } W\left\{\frac{D}{K}\exp\left\{\frac{D}{K} - \frac{\beta}{K}\tau\right\}\right\} + \tilde{\sigma}.$$

Using the properties of the Lambert W function and the chain rule, we obtain

$$F'(D) = \frac{(K+D)\text{ Lambert } W\left\{\frac{D}{K}\exp\left\{\frac{D}{K} - \frac{\beta}{K}\tau\right\}\right\}}{D\left(1 + \text{Lambert } W\left\{\frac{D}{K}\exp\left\{\frac{D}{K} - \frac{\beta}{K}\tau\right\}\right\}\right)}. \tag{3.9}$$

The stability analysis yields:

(i) If $|F'(D^*)| < 1$, the periodic solution $\tilde{D}(t)$ is locally asymptotically stable;

(ii) if $|F'(D^*)| > 1$, $\tilde{D}(t)$ becomes unstable.

From (3.9), it follows that

$$F'(D^*) = \frac{(K + D^*)\,\text{Lambert } W\left\{\frac{D^*}{K}\exp\left\{\frac{D^*}{K} - \frac{\beta}{K}\tau\right\}\right\}}{D^*\left(1 + \text{Lambert } W\left\{\frac{D^*}{K}\exp\left\{\frac{D^*}{K} - \frac{\beta}{K}\tau\right\}\right\}\right)}. \tag{3.10}$$

Moreover, since the principal branch of the Lambert W function is strictly increasing and satisfies $W(x) > -1$ for all $x > -\exp\{-1\}$, we have

$$1 + \text{Lambert } W\left\{\frac{D^*}{K}\exp\left\{\frac{D^*}{K} - \frac{\beta}{K}\tau\right\}\right\} > 0.$$

The condition $|F'(D^*)| < 1$, is equivalent to

$$\left|\frac{(K + D^*)\,\text{Lambert } W\left\{\frac{D^*}{K}\exp\left\{\frac{D^*}{K} - \frac{\beta}{K}\tau\right\}\right\}}{D^*}\right| < 1 + \text{Lambert } W\left\{\frac{D^*}{K}\exp\left\{\frac{D^*}{K} - \frac{\beta}{K}\tau\right\}\right\}, \tag{3.11}$$

which automatically implies both

$$\frac{(K + D^*)\text{Lambert } W\left\{\frac{D^*}{K}\exp\left\{\frac{D^*}{K} - \frac{\beta}{K}\tau\right\}\right\}}{D^*} < 1 + \text{Lambert } W\left\{\frac{D^*}{K}\exp\left\{\frac{D^*}{K} - \frac{\beta}{K}\tau\right\}\right\}, \tag{3.12}$$

and

$$\frac{(K + D^*)\text{Lambert } W\left\{\frac{D^*}{K}\exp\left\{\frac{D^*}{K} - \frac{\beta}{K}\tau\right\}\right\}}{D^*} > -1 - \text{Lambert } W\left\{\frac{D^*}{K}\exp\left\{\frac{D^*}{K} - \frac{\beta}{K}\tau\right\}\right\}. \tag{3.13}$$

From (3.11), we further obtain

$$\frac{K}{D^*}\,\text{Lambert } W\left\{\frac{D^*}{K}\exp\left\{\frac{D^*}{K} - \frac{\beta}{K}\tau\right\}\right\} < 1. \tag{3.14}$$

Under the condition $\tilde{\sigma}/\beta < \tau$, the positive fixed point D^* satisfies

$$\frac{D^*}{K} - \frac{\tilde{\sigma}}{K} = \text{Lambert } W\left\{\frac{D^*}{K}\exp\left\{\frac{D^*}{K} - \frac{\beta}{K}\tau\right\}\right\}.$$

By algebraic manipulation, this implies

$$\frac{K}{D^*}\,\text{Lambert } W\left\{\frac{D^*}{K}\exp\left\{\frac{D^*}{K} - \frac{\beta}{K}\tau\right\}\right\} = \frac{D^* - \tilde{\sigma}}{D^*} < 1.$$

Therefore, inequality (3.11) holds whenever $\tilde{\sigma}/\beta < \tau$. The second inequality(3.12) is trivially satisfied due to positivity. We conclude that difference equation (3.4) possesses a unique locally asymptotically stable positive fixed point provided that $\tilde{\sigma}/\beta < \tau$. □

Theorem 3.4. (Global attractivity) *If $D^* > 0$ is the unique positive fixed point of difference equation* (3.4)*, then every solution $D(t)$ of system* (3.1) *converges to $\tilde{D}(t)$ as $t \to \infty$. This shows that $\tilde{D}(t)$ is globally asymptotically stable.*

Proof. When $F'(D) = 0$, a critical point is given by $D_1 = -K$, and it follows that

$$D^* > 0 > D_1.$$

Define the n-th iterate

$$F^n(D) = F(F^{n-1}(D)), \qquad n = 2, 3, ...$$

Case 1. For any $D_2 \in (0, D^*]$, the sequence $\{F^n(D)\}$ is strictly increasing. Since $D_2 < F(D_2) < D^*$, the iterates satisfy

$$F^{n-1}(D_2) < F^n(D_2) < \cdots < D^*,$$

which implies

$$F^n(D_2) \xrightarrow{n\to\infty} D^*.$$

Case 2. For any $D_2 \in [D^*, +\infty)$, the sequence is strictly decreasing. Indeed, since $D^* < F(D_2) < D_2$ and $D^* < F^2(D_2) < F(D_2)$, we obtain

$$F^n(D_2) \xrightarrow{n\to\infty} D^*.$$

Combining both cases, we conclude that

$$\lim_{n\to\infty} F^n(D_2) = D^*$$

and hence

$$\lim_{t\to\infty} D(t) = \tilde{D}(t).$$

Thus, $\tilde{D}(t)$ is globally attractive, For any $\varepsilon_1 > 0$, there exists $T > 0$ such that for all $t > T$, the inequality

$$\tilde{D}(t) - \varepsilon_1 \le D(t) \le \tilde{D}(t) + \varepsilon_1, \tag{3.15}$$

holds. Therefore, system (3.1) admits a globally asymptotically stable periodic solution. In particular, for every solution $D(t)$ of system (3.1), we have

$$D(t) \to \tilde{D}(t)$$

as $t \to \infty$, $\quad t \in (n\tau, (n+1)\tau]$, $n \in \mathbb{Z}_+$. Using the method described in [10, 15, 18, 38], when $\frac{\tilde{\sigma}}{\tilde{\beta}} < \tau$, system (1.2) exhibits a positive tumor free periodic solution

$$(0, \tilde{D}(t)) = \left(0, K \text{ Lambert } W\left\{\frac{D^*}{K}\exp\left\{\frac{D^*}{K} - \frac{\beta}{K}(t - n\tau)\right\}\right\}\right) \tag{3.16}$$

for $t \in (n\tau, (n+1)\tau$ with $n \in \mathbb{Z}_+$. □

The conditions under which the positive tumor free periodic solution $(0, \tilde{D}(t))$ is globally asymptotically stable will now be discussed.

Theorem 3.5. *The tumor free periodic solution* $(0, \tilde{D}(t))$ *of system* (1.2) *is locally asymptotically stable provided that*

$$r\tau - \alpha\tau - k\int_0^\tau K \text{ Lambert } W\left(\frac{D^*}{K}\exp\left\{\frac{D^*}{K} - \frac{\beta}{K}t\right\}\right) dt < 0.$$

Furthermore, $(0, \tilde{D}(t))$ *is globally asymptotically stable if*

$$r\tau - \frac{\alpha}{1+\omega M_0}\tau - k\int_0^\tau K \text{ Lambert } W\left(\frac{D^*}{K}\exp\left\{\frac{D^*}{K} - \frac{\beta}{K}t\right\}\right) dt < 0. \tag{3.17}$$

Proof. To analyze the local stability of the tumor-free periodic solution $(0, \tilde{D}(t))$, we linearize system (1.2) around this solution. Let $H(t) = u(t)$ and $D(t) = v(t) + \tilde{D}(t)$. Then, the fundamental matrix $\Phi(t)$ associated with the linearized system satisfies

$$\frac{d\Phi}{dt} = \begin{pmatrix} r - \alpha - k\tilde{D}(t) & 0 \\ 0 & -\dfrac{\beta K}{(K + \tilde{D}(t))^2} \end{pmatrix} \Phi(t), \qquad \Phi(0) = I,$$

where I is the identity matrix. Integrating yields

$$\Phi(t) = \begin{pmatrix} \exp\left\{\displaystyle\int_0^t (r - \alpha - k\tilde{D}(t))\, dt\right\} & 0 \\ 0 & \exp\left\{\displaystyle\int_0^t -\frac{\beta K}{(K + \tilde{D}(t))^2}\, dt\right\} \end{pmatrix}. \tag{3.18}$$

From the impulse conditions of system (1.2), we obtain

$$B = \begin{pmatrix} 1 & 0 \\ 0 & 1 \end{pmatrix},$$

so the matrix is

$$M = B\Phi(\tau) = \begin{pmatrix} \exp\left\{\displaystyle\int_0^\tau (r - \alpha - k\tilde{D}(t))\, dt\right\} & 0 \\ 0 & \exp\left\{\displaystyle\int_0^\tau -\frac{\beta K}{(K + \tilde{D}(t))^2}\, dt\right\} \end{pmatrix}. \tag{3.19}$$

By Floquet theory, the eigenvalues of M (the Floquet multipliers) determine local stability:

$$|\mu_1| = \exp\left\{\int_0^\tau -\frac{\beta K}{(K + \tilde{D}(t))^2}\, dt\right\} < 1,$$
$$|\mu_2| = \exp\left\{r\tau - \alpha\tau - k\int_0^\tau K \,\text{Lambert } W\left(\frac{D^*}{K}\exp\left\{\frac{D^*}{K} - \frac{\beta}{K}t\right\}\right) dt\right\} < 1.$$

Clearly, $|\mu_1| < 1$. Thus, the tumor free periodic solution is locally asymptotically stable if $|\mu_2| < 1$, which holds under the stated condition with $D^* = \frac{\tilde{\sigma}}{1 - \exp\left\{\frac{1}{K}(\tilde{\sigma} - \beta\tau)\right\}}$. For global stability, we utilize the global attractivity of $\tilde{D}(t)$ (see (3.15)). There exists $\varepsilon_1 > 0$, such that

$$\tilde{D}(t) - \varepsilon_1 \le D(t) \le \tilde{D}(t) + \varepsilon_1,$$

for all $t > T$. Using the boundedness of $H(t)$, we derive the comparison system

$$\begin{cases} \dfrac{dH}{dt} \le rH(t) - \dfrac{\alpha}{1 + \omega M_0} H(t) - k\big(\tilde{D}(t) - \varepsilon_1\big)H(t), & t \ne n\tau, \\ H(t^+) = H(t), & t = n\tau, \end{cases} \tag{3.20}$$

which implies that for $t \in (n\tau, (n+1)\tau]$,

$$H((n+1)\tau) \le H(n\tau^+) \exp\left\{\int_{n\tau}^{(n+1)\tau} \left(r - \frac{\alpha}{1 + \omega M_0} - k(\tilde{D}(t) - \varepsilon_1)\right) dt\right\}$$
$$= H(n\tau)\rho.$$

If

$$r\tau - \frac{\alpha}{1+\omega M_0}\tau + k\varepsilon_1\tau - k\int_0^\tau K\,\text{Lambert } W\left(\frac{D^*}{K}\exp\left\{\frac{D^*}{K} - \frac{\beta}{K}t\right\}\right)dt < 0,$$

then $H(n\tau) \le H(0^+)\rho^n$, and hence $H(n\tau) \to 0$ as $t \to \infty$. Since

$$0 < H(t) < H(n\tau)\exp(r\tau), \quad t \in (n\tau, (n+1)\tau],$$

we conclude $H(t) \to 0$ as $t \to \infty$. Therefore, $(0, \tilde{D}(t))$ is globally asymptotically stable under condition (3.17). □

Biological interpretation. Theorem 3.5 shows that the tumor-free state $(0, \tilde{D}(t))$ is stable when the combined effects of the immune response and chemotherapy dominate the intrinsic growth of tumor cells. small perturbations in the tumor cell population decay over time, ensuring tumor elimination. Globally, all solutions of the system converge to the extinction state if the inhibitory effects of the immune system and treatment are sufficiently strong, thereby guaranteeing the long-term eradication of the tumor.

4. Permanence

In clinical oncology practice, cancer therapy does not necessarily demand the complete eradication of tumor cells. From a translational standpoint, it is often more clinically meaningful to identify the reciprocal regulatory mechanisms that allow tumor cells and the host's healthy tissues to coexist. Such a balance emphasizes preserving patient quality of life while maintaining control over disease progression. Motivated by this perspective, we now turn to investigating the permanence of the proposed tumor–therapy dynamical system, with the goal of providing theoretical foundations for designing clinically feasible treatment regimens that support stable coexistence.

Theorem 4.1. *if*

$$r\tau - \alpha\tau - k\int_0^\tau K\,\textit{Lambert } W\left(\frac{D^*}{K}\exp\left\{\frac{D^*}{K} - \frac{\beta}{K}t\right\}\right)dt > 0 \tag{4.1}$$

where $D^* = \frac{\tilde{\sigma}}{1-\exp\left\{\frac{1}{K}(\tilde{\sigma}-\beta\tau)\right\}}$, *system* (1.2) *is permanent.*

Proof. Assume that $H(t)$ and $D(t)$ are positive solutions to system (1.2), with $H(t) > 0$ and $D(t) > 0$ for all $t \ge 0$. From the boundedness of solutions, we deduce that $H(t) < M_0$, where M_0 is a constant. By condition (3.12), there exist constants $m_2, M_2 > 0$ such that

$$m_2 \le D(t) \le M_2, \tag{4.2}$$

where

$$m_2 = \inf_{t>0}\tilde{D}(t) - \varepsilon_1 = K\,\text{Lambert } W\left\{\frac{D^*}{K}\exp\left\{\frac{D^*}{K} - \frac{\beta}{K}\tau\right\}\right\} - \varepsilon_1,$$

$$M_2 = \sup_{t>0}\tilde{D}(t) + \varepsilon_1 = K\,\text{Lambert } W\left\{\frac{D^*}{K}\exp\left\{\frac{D^*}{K}\right\}\right\} + \varepsilon_1.$$

(i) By (4.1), select $\varepsilon_1 > 0$ and $m_1 > 0$ sufficiently small such that

$$\zeta_1 \triangleq \exp\left\{r\tau - \alpha\tau - r\eta m_1\tau - k\varepsilon_1\tau - k\int_0^\tau K\,\text{Lambert } W\left(\frac{D^*}{K}\exp\left(\frac{D^*}{K} - \frac{\beta}{K}t\right)dt\right\}\right\} > 1. \tag{4.3}$$

Suppose, for the sake of contradiction, that $H(t) < m_1$ for all $t > 0$. Then, the corresponding impulsive differential system (1.2) satisfies

$$\begin{cases} \dfrac{dH}{dt} \geq H(t)\left(r - r\eta m_1 - \alpha - k(\tilde{D}(t) + \varepsilon_1)\right), & t \neq n\tau, \\ H(t^+) = H(t), & t = n\tau, \end{cases} \tag{4.4}$$

for $t > \tau_0$. Let $N \in \mathbb{Z}_+$ with $N\tau > \tau_0$. Integrating equation (4.4) over $t \in (n\tau, (n+1)\tau]$ for $n > N$ gives

$$H((n+1)\tau) \geq H(n\tau^+)\exp\left\{\int_{n\tau}^{(n+1)\tau}\left(r - r\eta m_1 - \alpha - k(\tilde{D}(t) + \varepsilon_1)\right)dt\right\} \geq H(n\tau)\zeta_1. \tag{4.5}$$

By recursion, we have

$$H((N+n)\tau) \geq H(N\tau)\zeta_1^n \to \infty$$

as $n \to \infty$. This leads to a contradicting the boundedness of $H(t)$. Therefore, there exists $t_1 > 0$ such that $H(t_1) \geq m_1$.

(ii) We now show that $H(t) \geq m_1$ for all $t > t_1$. Assume otherwise, and define $\hat{t} = \inf_{t>t_1}\{H(t) \leq m_1\}$. there exists large enough t_2, integrating equation (4.4) over $t \in (\hat{t}, t_2]$ yields

$$H(t_2) \geq H(\hat{t}^+)\exp\left\{\int_{\hat{t}}^{t_2}\left(r - r\eta m_1 - \alpha - k(\tilde{D}(t) + \varepsilon_1)\right)dt\right\} \geq H(\hat{t}^+)\zeta_1. \tag{4.6}$$

Since $\zeta_1 > 1$, such that $H(t_2) > m_1$. Let

$$t^* = \inf_{t>t_1}\{H(t) > m_1\}.$$

Then, for $t \in (\hat{t}, t^*)$, we have $H(t) \leq m_1$ and $H(t^*) = m_1$. From equation (4.4), it follows that

$$\begin{aligned} H(t) &\geq H(\hat{t}^+)\exp\left\{\int_{\hat{t}}^{t^*}\left(r - r\eta m_1 - \alpha - k(\tilde{D}(t) + \varepsilon_1)\right)dt\right\} \\ &= m_1\exp\left\{\int_{\hat{t}}^{t^*}\left(r - r\eta m_1 - \alpha - k(\tilde{D}(t) + \varepsilon_1)\right)dt\right\} \\ &= m_3, \end{aligned} \tag{4.7}$$

for all $t \in (\hat{t}, t^*)$. Hence, $H(t) \geq m_3$ in this interval. By applying an analogous argument for $t > t^*$, we conclude that $H(t) \geq m_0 = \min\{m_1, m_3\}$ for all $t > t_1$. □

Remark 4.1. The global stability conditions for the tumor-free periodic solution are closely related to the permanence conditions. To investigate how these conditions shape the dynamical behavior of system (1.2), we introduce the quantities R_1 and R_2 as follows.

$$R_1 = r\tau - \frac{\alpha}{1 + \omega M_0}\tau - k\int_0^\tau K\,\text{Lambert } W\left(\frac{D^*}{K}\exp\left\{\frac{D^*}{K} - \frac{\beta}{K}t\right\}\right)dt,$$

$$R_2 = r\tau - \alpha\tau - k\int_0^\tau K\,\text{Lambert } W\left(\frac{D^*}{K}\exp\left\{\frac{D^*}{K} - \frac{\beta}{K}t\right\}\right)dt.$$

From Theorem 3.5 and Theorem 4.1, it follows that $R_2 < R_1$. Consequently,

(i) if $R_2 < R_1 < 0$, the tumor-free periodic solution of system (1.2) is locally asymptotically stable;

(ii) if $0 < R_2 < R_1$, then system (1.2) is permanent.

5. Existence and stability of positive periodic solution

In this section, we carry out a comprehensive analysis of the two critical conditions to clarify how the interaction between intrinsic system parameters and impulsive effects governs the stability of system (1.2). We have established that when

$$r\tau - \alpha\tau - k\int_0^\tau K\,\text{Lambert } W\left(\frac{D^*}{K}\exp\left\{\frac{D^*}{K} - \frac{\beta}{K}t\right\}\right)dt > 0,$$

the tumor-free periodic solution loses stability. To further investigate the dynamical behavior of the system following this loss of stability, we employ bifurcation theory.

Theorem 5.1. *If*

$$d' = 1 - \exp\left\{r\tau_0 - \alpha\tau_0 - k\int_0^{\tau_0}\tilde{D}(t)\,dt\right\} = 0,$$

then system (1.2) *admits a positive non-trivial periodic solution. Moreover, if*

$$\frac{\beta K}{(K+\tilde{D}_{\max})^2}\tau_0 > \ln\left(1 + \frac{\alpha\omega - r\eta}{k}\right),$$

this non-trivial periodic solution is supercritical.

Proof. First, we derive the bifurcation of nontrivial periodic solutions in the neighborhood of $(0, \tilde{D}(t))$. For computational convenience, let $\chi(t) = H(t)$ and $\gamma(t) = D(t)$. Then, system (1.2) is transformed into

$$\left\{\begin{array}{l} \left.\begin{array}{l} \dfrac{d\gamma}{dt} = -\dfrac{\beta\gamma(t)}{K+\gamma(t)} \\ \dfrac{d\chi}{dt} = r\chi(t)(1-\eta\chi(t)) - \dfrac{\alpha\chi(t)}{1+\omega\chi(t)} - k\gamma(t)\chi(t) \end{array}\right\} t \neq n\tau, \\ \left.\begin{array}{l} \gamma(t^+) = \gamma(t) + \tilde{\sigma} \\ \chi(t^+) = \chi(t) \end{array}\right\} t = n\tau. \end{array}\right. \tag{5.1}$$

Φ is the flow of the equation, and $X_t = \Phi(t, X_0)$, F is the solution of the unperturbed system, while Θ represents the mapping at pulse instants [12, 14, 26]. We use the following expressions to represent the right-hand side of the system

$$F_1(\gamma,\chi) = -\frac{\beta\gamma(t)}{K+\gamma(t)},$$

$$F_2(\gamma,\chi) = r\chi(t)(1-\eta\chi(t)) - \frac{\alpha\chi(t)}{1+\omega\chi(t)} - k\gamma(t)\chi(t),$$

$$\Theta_1(\gamma,\chi)=\gamma(t)+\tilde{\sigma},$$
$$\Theta_2(\gamma,\chi)=\chi(t),$$
$$\zeta(t)=(X_s(0),0)=(\tilde{D}(t),0).$$

The bifurcation theory and related techniques described in [14] are applied to obtain the non-trivial periodic solutions of the system. The bifurcation phenomena near the boundary periodic solutions $(X_s(0),0)$ of the system are studied. The variational equations for the systems are as follows

$$\frac{d}{dt}\big(D_x(\Theta(t,X_0))\big)=D_xF\big(D_x(\Theta(t,X_0))\big)\big(D_x(\zeta(t,X_0))\big),$$

where $D_x(\Theta(t,X_0))=I$, and variational equation form corresponding to system (5.1) is

$$\begin{aligned}\frac{d}{dt}\begin{pmatrix}\frac{\partial\Phi_1}{\partial\gamma} & \frac{\partial\Phi_1}{\partial\chi}\\ \frac{\partial\Phi_2}{\partial\gamma} & \frac{\partial\Phi_2}{\partial\chi}\end{pmatrix}(t,X_0)&=\begin{pmatrix}\frac{\partial F_1(\zeta(t))}{\partial\gamma} & \frac{\partial F_1(\zeta(t))}{\partial\chi}\\ \frac{\partial F_2(\zeta(t))}{\partial\gamma} & \frac{\partial F_2(\zeta(t))}{\partial\chi}\end{pmatrix}\begin{pmatrix}\frac{\partial\Phi_1}{\partial\gamma} & \frac{\partial\Phi_1}{\partial\chi}\\ \frac{\partial\Phi_2}{\partial\gamma} & \frac{\partial\Phi_2}{\partial\chi}\end{pmatrix}(t,X_0)\\ &=\begin{pmatrix}-\frac{\beta K}{(K+\tilde{D}(t))^2} & 0\\ 0 & r-\alpha-k\tilde{D}(t)\end{pmatrix}\begin{pmatrix}\frac{\partial\Phi_1}{\partial\gamma} & \frac{\partial\Phi_1}{\partial\chi}\\ \frac{\partial\Phi_2}{\partial\gamma} & \frac{\partial\Phi_2}{\partial\chi}\end{pmatrix}(t,X_0),\end{aligned}$$

with $\frac{\partial\Phi_2(0,X_0)}{\partial\gamma}=0$, integrating the above expression yields

$$\frac{\partial\Phi_2(t,X_0)}{\partial\gamma}=\exp\Big\{\int_0^t r-\alpha-k\tilde{D}(t)dt\Big\}\frac{\partial\Phi_2(0,X_0)}{\partial\gamma}=0,$$

applying the initial condition $D_X(\Phi(0,X_0))=E_2$ for $t\in(0,\tau]$, the solution is expressed as

$$\begin{aligned}\frac{\partial\Phi_2(t,X_0)}{\partial\chi}&=\rho(t),\\ \frac{\partial\Phi_1(t,X_0)}{\partial\gamma}&=\exp\Big\{\int_0^t-\frac{\beta K}{(K+\tilde{D}(t))^2}dt\Big\},\\ \frac{\partial\Phi_1(t,X_0)}{\partial\chi}&=\exp\left\{\int_0^t-\frac{\beta K}{(K+\tilde{D}(t))}dt\right\},\end{aligned}$$

where $\rho(t)=\exp\left\{\int_0^t r-\alpha-k\tilde{D}(u)du\right\}$, hence we have

$$\begin{aligned}a'&=(1-\frac{\partial\Theta_1}{\partial\gamma}\frac{\partial\Phi_1}{\partial\gamma})_{(\tau_0,X_0)}=1-\exp\Big\{\int_0^{\tau_0}-\frac{\beta K}{(K+\tilde{D}(t))^2}dt\Big\}>0,\\ b'&=-\exp(\frac{\partial\Theta_1}{\partial\gamma}\frac{\partial\Phi_1}{\partial\chi}+\frac{\partial\Theta_1}{\partial\chi}\frac{\partial\Phi_2}{\partial\chi})_{(\tau_0,X_0)}=-\exp\Big\{\int_0^{\tau_0}-\frac{\beta K}{(K+\tilde{D}(t))^2}dt\Big\},\\ c'&=0,\\ d'&=(1-\frac{\partial\Theta_2}{\partial\chi}\frac{\partial\Phi_2}{\partial\chi})_{(\tau_0,X_0)}=1-\exp\left\{r\tau_0-\alpha\tau_0-k\int_0^{\tau_0}\tilde{D}(t)dt\right\}=1-\rho(\tau_0).\end{aligned}$$

Let $d^{'}$ be the bifurcation parameter of the dynamical system. When $d^{'}=0$, the system possesses a supercritical bifurcation, and the critical parameter value satisfies $\rho(\tau_0)=1$. Considering the initial condition $\frac{\partial^2\Phi_2(0,X_0)}{\partial\gamma^2}=0$ and $\frac{\partial^2\Phi_2(0,X_0)}{\partial\gamma\partial\chi}=0$, solving the integral of the above equation yields

$$\begin{aligned}
\frac{\partial^2\Phi_2(\tau_0,X_0)}{\partial\gamma\partial\chi}=&\int_0^{\tau_0}\exp\left\{\int_u^{\tau_0}\frac{\partial F_2(\tilde{D}(t),0)}{\partial\chi}dt\right\}\frac{\partial^2F_2(\tilde{D}(t),0)}{\partial\gamma\partial\chi}\exp\left\{\int_0^{u}\frac{\partial F_2(\tilde{D}(t),0)}{\partial\chi}dt\right\}du\\
=&-k\int_0^{\tau_0}\exp\Big\{\int_0^{\tau_0}r-\alpha-K\tilde{D}(u)du\Big\}du\\
=&-k\tau_0\\
<&0,\\
\frac{\partial^2\Phi_2(\tau_0,X_0)}{\partial\tau\partial\chi}=&\frac{\partial F_2(\tilde{D}(t),0)}{\partial\chi}\exp\left\{\int_0^{\tau_0}\frac{\partial F_2(\tilde{D}(t),0)}{\partial\chi}dt\right\}\\
=&(r-\alpha-k\tilde{D}(t))\exp\left\{\int_0^{\tau_0}r-\alpha-k\tilde{D}(t)dt\right\}\\
=&r-\alpha-k\tilde{D}(t)\rho(\tau_0)\\
=&r-\alpha-k\tilde{D}(t),\\
\frac{\partial^2\Phi_2(\tau_0,X_0)}{\partial\chi^2}=&\int_0^{\tau_0}\exp\left\{\int_u^{\tau_0}\frac{\partial F_2(\tilde{D}(t),0)}{\partial\chi}dt\right\}\frac{\partial^2F_2(\tilde{D}(t),0)}{\partial\chi^2}\exp\left\{\int_0^{u}\frac{\partial F_2(\tilde{D}(t),0)}{\partial\chi}dt\right\}du\\
&+\int_0^{\tau_0}\exp\left\{\int_u^{\tau_0}\frac{\partial F_2(\tilde{D}(t),0)}{\partial\chi}dt\right\}\frac{\partial^2F_2(\tilde{D}(t),0)}{\partial\chi\partial\gamma}\int_0^{u}\exp\left\{\int_g^{u}\frac{\partial F_1(\tilde{D}(t),0)}{\partial\gamma}du\right\}\\
&\times\frac{\partial F_1(\tilde{D}(t),0)}{\partial\chi}\exp\left\{\int_0^{g}\frac{\partial F_2(\tilde{D}(t),0)}{\partial\chi}dt\right\}dg\\
=&\int_0^{\tau_0}(-2r\eta+2\alpha\omega)\exp\left\{\int_0^{\tau_0}r-\alpha-k\tilde{D}(t)dt\right\}du\\
=&\int_0^{\tau_0}(-2r\eta+2\alpha\omega)\,\rho(\tau_0)du\\
=&2\,(\alpha\omega-r\eta)\,\tau_0.
\end{aligned}$$

After calculation, we obtain $\frac{\partial\Theta_1}{\partial\chi}=\frac{\partial\Theta_2}{\partial\gamma}=0,\frac{\partial\Theta_1}{\partial\gamma}=\frac{\partial\Theta_2}{\partial\chi}=1,\frac{\partial^2\Theta_i}{\partial\gamma\partial\chi}=0$ for $i=1,2$ and $\frac{\partial^2\Theta_i}{\partial^2\gamma}=\frac{\partial^2\Theta_i}{\partial^2\chi}=0$. Thus we obtain the expressions for B and C respectively

$$\begin{aligned}
B=&\frac{\partial^2\Theta_2}{\partial\gamma\partial\chi}\left(\frac{\partial\Phi_1(\tau_0,X_0)}{\partial\tau}+\frac{\partial\Phi_1(\tau_0,X_0)}{\partial\gamma}\frac{1}{a'}\frac{\partial\Theta}{\partial\gamma}\frac{\partial\Theta_1(\tau_0,X_0)}{\partial\tau}\right)\frac{\partial\Theta_2(\tau_0,X_0)}{\partial\chi}\\
&-\frac{\partial\Theta_2}{\partial\chi}\left(\frac{\partial^2\Phi_2(\tau_0,X_0)}{\partial\gamma\partial\chi}\frac{1}{a'}\frac{\partial\Theta_1}{\partial\gamma}\frac{\partial\Phi_1(\tau_0,X_0)}{\partial\tau}+\frac{\partial^2\Phi_2(\tau_0,X_0)}{\partial\tau\partial\chi}\right)\\
=&-\left(-k\tau_0\frac{1}{a'}\tilde{D}'(t)+r-\alpha-k\tilde{D}(t)\right),\\
C=&-2\frac{\partial^2\Theta_2}{\partial\chi\partial\gamma}\left(-\frac{b'}{a'}\frac{\partial\Phi_1(\tau_0,X_0)}{\partial\gamma}+\frac{\partial\Phi_1(\tau_0,X_0)}{\partial\chi}\right)\frac{\partial\Phi_2(\tau_0,X_0)}{\partial\chi}
\end{aligned}$$

$$
\begin{aligned}
&- \frac{\partial^2 \Theta_2}{\partial \chi^2}\left(\frac{\partial \Phi_2(\tau_0, X_0)}{\partial \chi}\right)^2 + 2\frac{a'}{b'}\frac{\partial \Theta_2}{\partial \chi}\frac{\partial^2 \Phi_2}{\partial \chi \partial \gamma} - \frac{\partial \Theta_2}{\partial \chi}\frac{\partial^2 \Phi_2}{\partial \chi^2} \\
&= -2k\tau_0 \frac{1 - \exp\left\{\int_0^{\tau_0} -\frac{\beta K}{(K+\tilde{D}(t))^2} dt\right\}}{-\exp\left\{\int_0^{\tau_0} -\frac{\beta K}{(K+\tilde{D}(t))^2} dt\right\}} - 2\left(\alpha\omega - r\eta\right)\tau_0 \\
&= -2k\tau_0\big(1 - \exp\{\int_0^{\tau_0} \frac{\beta K}{(K+\tilde{D}(t))^2} dt\}\big) - 2\left(\alpha\omega - r\eta\right)\tau_0.
\end{aligned}
$$

Under the permanence condition, we rigorously establish that $r-\alpha-k\tilde{D}(t) > 0$. We need to determine the sign of $\tilde{D}'(t)$. According to the properties of the Lambert W function, we have

$$
\tilde{D}'(t) = -\frac{\beta}{K} \cdot \frac{(K + D^*)\,\text{Lambert } W\left(\frac{D^*}{K}\exp\left\{\frac{D^*}{K} - \frac{\beta}{K}(t - n\tau)\right\}\right)}{D^*\left(1 + \text{Lambert } W\left(\frac{D^*}{K}\exp\left\{\frac{D^*}{K} - \frac{\beta}{K}(t - n\tau)\right\}\right)\right)} < 0,
$$

hence $(-k\tilde{D}'(t) + r - \alpha - k\tilde{D}(t)) > 0$, leading to the conclusion that $B < 0$. The sign of C is now determined. Given that $\tilde{D}(t)$ is monotonically decreasing in$t$, according to (3.8), the maximum value of $\tilde{D}(t)$ is attained as

$$
\tilde{D}_{\max} = K\,\text{Lambert } W\left(\frac{D^*}{K}\exp\left\{\frac{D^*}{K} + \frac{\beta n\tau}{K}\right\}\right).
$$

Considering the expression of C, $C > 0$ is equivalent to

$$
\exp\left(\int_0^{\tau_0} \frac{\beta K}{(K+\tilde{D}(t))^2} dt\right) > \ln\left(1 + \frac{\alpha\omega - r\eta}{k}\right).
$$

If $\frac{\beta K}{\kappa + \tilde{D}_{\max}}\tau_0 > \ln\left(1 + \frac{\alpha\omega - r\eta}{k}\right)$ additionally holds, then $C > 0$. It is derived from the theorem that system (1.2) undergoes a supercritical bifurcation at $d^* = 0$. □

6. Numerical simulation

This section aims to validate the effectiveness and rationality of the fixed-time external injection therapy strategy for chemotherapeutic agents under a nonlinear degradation rate. To improve the clarity of the numerical part, we first emphasize that the parameter sets used in the simulations are chosen to represent biologically reasonable treatment scenarios and to display the typical dynamical regimes predicted by the theoretical analysis, rather than to provide patient-specific fitted data. The analysis demonstrates that the relationship between the parameters R_1, R_2, and 0 directly determines the long-term dynamical state of the system. Numerical verification results are presented as follows.

Case 1. $R_1 < R_2 < 0$**.** Figure 2(a) shows that, under different initial conditions, the tumor cell concentration converges to the extinction state. Figure 2(b) illustrates that when the parameter condition $\frac{\beta}{\tau} > \tilde{\sigma}$ holds, the chemotherapeutic agent concentration converges to a globally asymptotically stable periodic solution, consistent with the conclusion of Theorem 3 and Theorem 4. Figure 2(c) further demonstrates the coupled interaction between the two variables: While tumor cells approach extinction, the chemotherapeutic agent still converges to a globally asymptotically stable periodic solution. This verifies Theorem 5, which guarantees the existence

of a periodic solution corresponding to tumor cell eradication in system (1.2). These results confirm that cancer cure can be achieved provided the dose of chemotherapeutic agent is reasonably controlled. It should be noted, however, that this stage of the analysis considers only the clearance effect of chemotherapeutic agents on tumor cells and does not account for their toxicity to normal human tissues.

From a biological perspective, this case represents a successful therapeutic scenario in which the combined suppressive effects of chemotherapy and baseline immune inhibition dominate the intrinsic tumor growth over each treatment cycle.

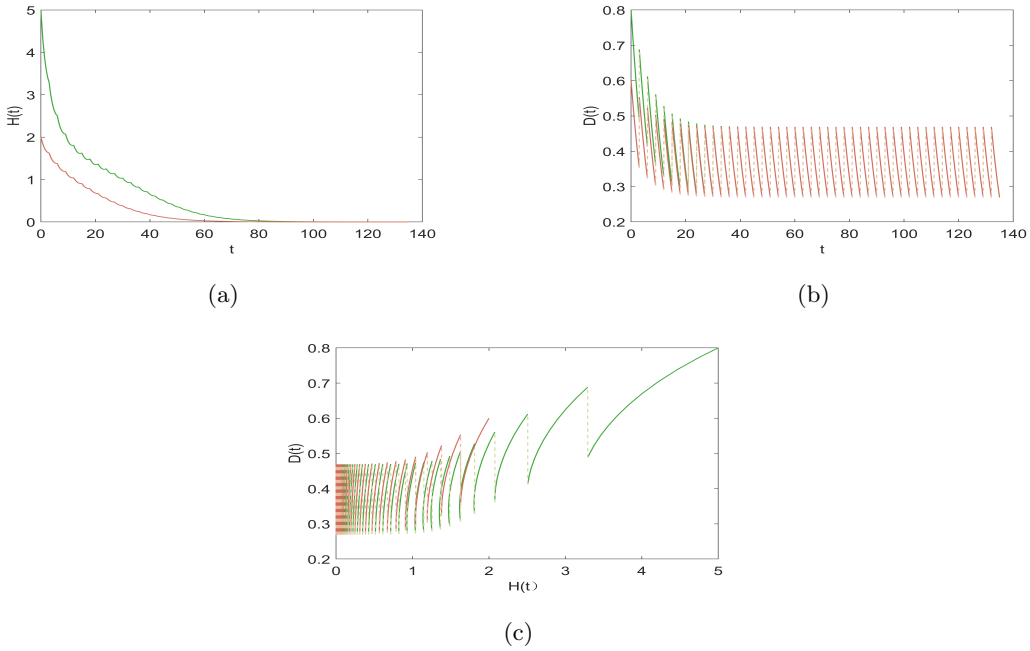

Figure 2. Periodic solutions for tumor eradication under different initial conditions: (a) Time series of tumor cell concentration $H(t)$: Both initial conditions $(H_0, D_0) = (5, 0.8)$ and $(H_0, D_0) = (2, 0.6)$ converge to 0, indicating tumor extinction. (b) Time series of drug concentration $D(t)$: The drug variable converges to a stable positive periodic solution. (c) Phase portrait of $H(t)$ vs. $D(t)$: Tumor cells approach extinction while drug concentration converges to the periodic solution, indicating convergence of the full system to the tumor-free periodic solution. Other parameters $r = 0.72$, $\alpha = 0.6$, $\eta = 0.05$, $\omega = 0.2$, $k = 0.6$, $\beta = 0.4$, $\tilde{\sigma} = 0.2$, $K = 1.8$, $\tau = 3$ [33].

Case 2. $0 < R_1 < R_2$**.** Figure 3 shows that, under different initial conditions, both tumor cell and chemotherapeutic agent concentrations converge to a stable periodic solution. This aligns with the conclusion of Theorem 6: Once the tumor-free periodic solution loses stability, the system enters a permanent state. Thus, cancer progression can still be effectively controlled by appropriately regulating the chemotherapeutic dose.

Biologically, this regime corresponds to chronic but controlled tumor management: Treatment is sufficient to prevent unbounded growth, but not strong enough to eliminate the tumor completely.

Case 3. $R_1 < 0 < R_2$**.** Figure 3 demonstrates that small perturbations in initial conditions may qualitatively change the trajectory of tumor cell concentration—from convergence to extinction to convergence toward a stable periodic solution. This suggests that the system may exhibit bistable behavior near the threshold region. Figure 3(a) shows that one initial condition leads to extinction, whereas another converges to a stable positive periodic solution. Figure 3(b)

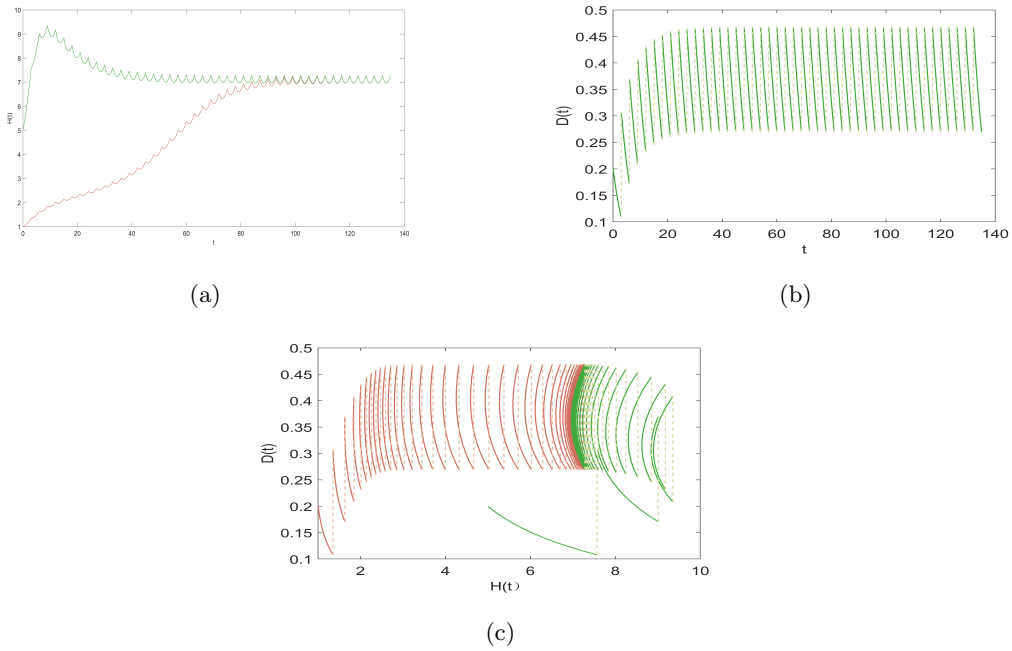

(a) (b)

(c)

Figure 3. Periodic solutions for tumor eradication under different initial conditions: (a) Time series of tumor cell concentration $H(t)$: Both initial conditions $(H_0, D_0) = (5, 0.8)$ and $(H_0, D_0) = (2, 0.6)$ converge to 0, indicating tumor extinction. (b) Time series of drug concentration $D(t)$: The drug variable converges to a stable positive periodic solution. (c) Phase portrait of $H(t)$ vs. $D(t)$: Tumor cells approach extinction while drug concentration converges to the periodic solution, indicating convergence of the full system to the tumor-free periodic solution. Other parameters $r = 0.72$, $\alpha = 0.6$, $\eta = 0.05$, $\omega = 0.2$, $k = 0.6$, $\beta = 0.4$, $\tilde{\sigma} = 0.2$, $K = 1.8$, $\tau = 3$ [33].

indicates that different initial drug levels produce different coupled system trajectories. Figure 3(c) reveals the coexistence of two distinct attractors in phase space, namely a tumor-free state and a positive limit cycle. Therefore, near this regime, baseline tumor burden and residual drug level may influence whether the system approaches eradication or only controlled permanence.

Clinical implications of dosing. In practical clinical applications, it is necessary to determine an optimal chemotherapeutic dose that suppresses tumor proliferation while minimizing toxicity to normal tissues. Figure 4(a) shows that when the injection dose is 0.2, the tumor cell concentration converges to a stable periodic solution. By contrast, when the dose is increased to 0.4 or 0.6, complete tumor eradication can be achieved. Figure 4(b) indicates that residual drug concentrations differ substantially across these three dosing levels: Higher doses yield greater residual concentrations, thereby increasing toxicity to normal tissues. This provides direct numerical evidence for dose optimization.

Figure 4 can be interpreted more systematically as follows. In Figure 4(a), increasing the impulsive dose drives the system from tumor permanence to tumor eradication, indicating that dose intensity is a key control parameter for long-term outcome. Figure 4(b) shows that higher doses produce larger residual drug concentrations throughout the treatment cycle, which may imply improved tumor suppression but also a potentially greater toxicity burden. Figure 4(c) further confirms this transition in phase space: The low-dose case approaches a positive periodic attractor, whereas the higher-dose cases converge to the tumor-free periodic solution. Thus, the model provides numerical support for the existence of a therapeutically relevant balance between efficacy and residual drug burden.

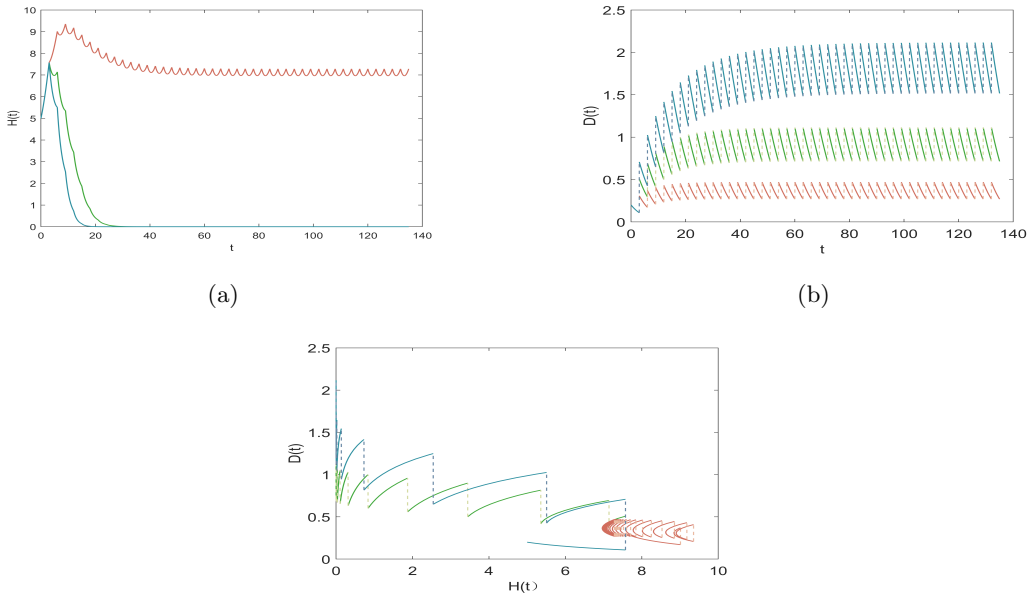

(a) (b) (c)

Figure 4. Dynamics under different injection doses. (a) Time series of tumor cell concentration $H(t)$: Red line ($\tilde{\sigma} = 0.2$) converges to a stable periodic solution; green line ($\tilde{\sigma} = 0.4$) and blue line ($\tilde{\sigma} = 0.6$) converge to extinction. (b) Time series of drug concentration $D(t)$: Higher doses lead to higher residual concentrations. (c) Phase portrait of $H(t)$ vs. $D(t)$: Dose-dependent dynamical transitions, providing numerical evidence for dose optimization. Initial condition: $(H_0, D_0) = (2, 0.4)$. Other parameters are the same as that in Figure 2.

Parameter sensitivity. The study further reveals that the model exhibits high sensitivity to parameter values, particularly to the intrinsic tumor growth rate r. As shown in Figure 5, even small variations in r can induce significant qualitative transitions in system dynamics. This observation highlights the importance of precise clinical measurement of parameter r and suggests that future studies should focus on improving the accuracy of its estimation.

More specifically, Figure 5(a) shows that a relatively small change in r can switch the long-term system behavior from tumor eradication to stable positive persistence. Figure 5(b) indicates that the influence of r on the drug profile itself is comparatively weak, whereas Figure 5(c) shows that the coupled phase dynamics still undergo a clear qualitative transition. These results indicate that tumor aggressiveness is a crucial determinant of whether a given treatment schedule is sufficient for eradication, even when the drug-related parameters remain unchanged.

Comparison of linear and nonlinear elimination rates. Figure 6 compares the evolutionary dynamics of tumor cells and chemotherapeutic agents under linear and nonlinear elimination rates, with the same initial conditions. Figure 6(a) shows that tumor evolution under the linear elimination rate is relatively simple. By contrast, under the nonlinear elimination rate, the chemotherapeutic agent exhibits a two-phase effect: An initial stimulation of tumor proliferation followed by inhibition under sustained exposure. This pattern more accurately reflects the pharmacodynamic process of drug action observed in clinical chemotherapy, demonstrating the superiority of the nonlinear elimination rate model in capturing clinical reality.

7. Conclusion and discussion

The core contribution of this study lies in developing an impulsive tumor chemotherapy model that explicitly characterizes the in vivo enzymatic degradation of chemotherapeutic agents via

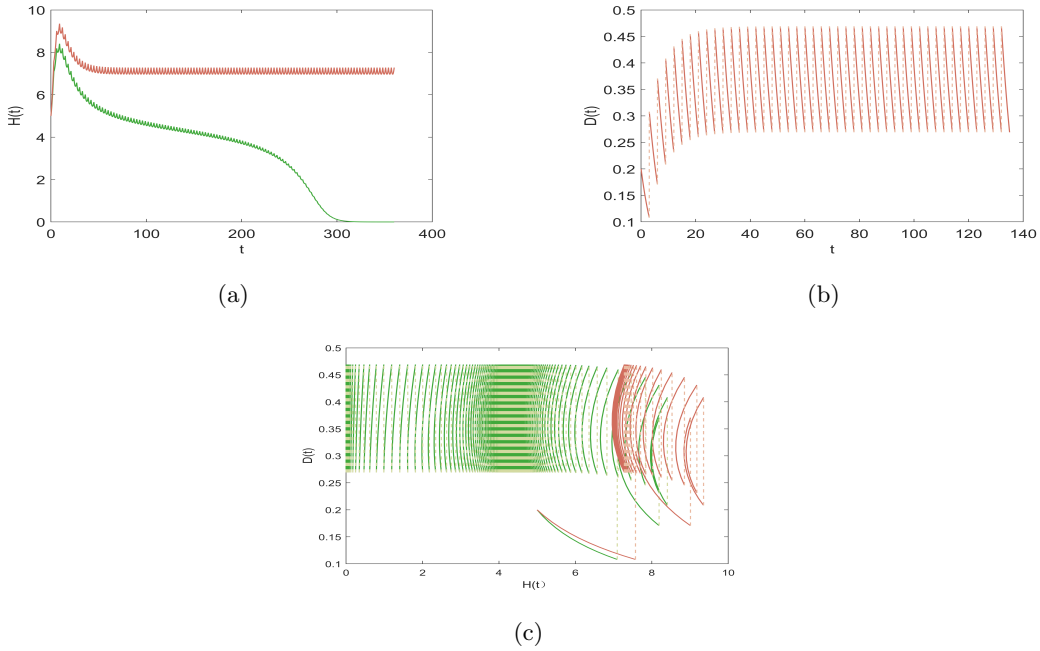

(a) (b) (c)

Figure 5. Sensitivity to parameter r (intrinsic tumor growth rate). (a) Time series of tumor cell concentration $H(t)$: Red line ($r = 0.72$) converges to extinction; green line ($r = 0.685$) converges to a stable positive periodic solution. (b) Time series of drug concentration $D(t)$: Parameter r has little effect on drug dynamics. (c) Phase portrait of $H(t)$ vs. $D(t)$: Small changes in r induce a qualitative transition in system dynamics. Initial condition: $(H_0, D_0) = (5, 0.2)$. Other parameters are the same as that in Figure 2.

Michaelis–Menten kinetics, thereby bridging the gap between idealized mathematical models and clinical practice. By employing the Lambert$W$ function, we derived explicit expressions for tumor-free periodic solutions and rigorously established their existence and boundedness. We further conducted a global stability analysis of the subsystem's fixed point and obtained two key analytical results: The global asymptotic stability condition (R_1) for tumor-free periodic solution (using Floquet theory and comparison principles) and the system's permanence condition (R_2). In addition, bifurcation analysis enriched the dynamical understanding of the system by uncovering stable positive periodic solutions and highlighting the critical role of initial values—directly linking the mathematics to clinically relevant factors such as residual drug levels and baseline tumor burden.

Compared with many existing tumor-treatment models based on continuous administration or linear pharmacokinetic decay, the present framework combines fixed-time impulsive chemotherapy with Michaelis–Menten nonlinear elimination, and therefore captures both the cyclic structure of treatment and the saturation effect of enzymatic drug clearance. In contrast to simpler linear-decay or purely continuous-treatment formulations, the model is able to describe threshold behavior between tumor eradication and permanence, as well as richer long-term dynamics such as stable periodic coexistence and bistability. In this sense, the present work extends earlier impulsive tumor-treatment models by emphasizing the coupling between nonlinear drug clearance and periodic treatment scheduling.

Numerical simulations corroborate these theoretical results. Consistent with conventional tumor models and basic dose–response theory, our simulations confirm that chemotherapeutic dose intensity is the dominant determinant of long-term therapeutic outcomes: Within safe ranges, higher doses effectively suppress tumor growth, whereas initial tumor burden exerts

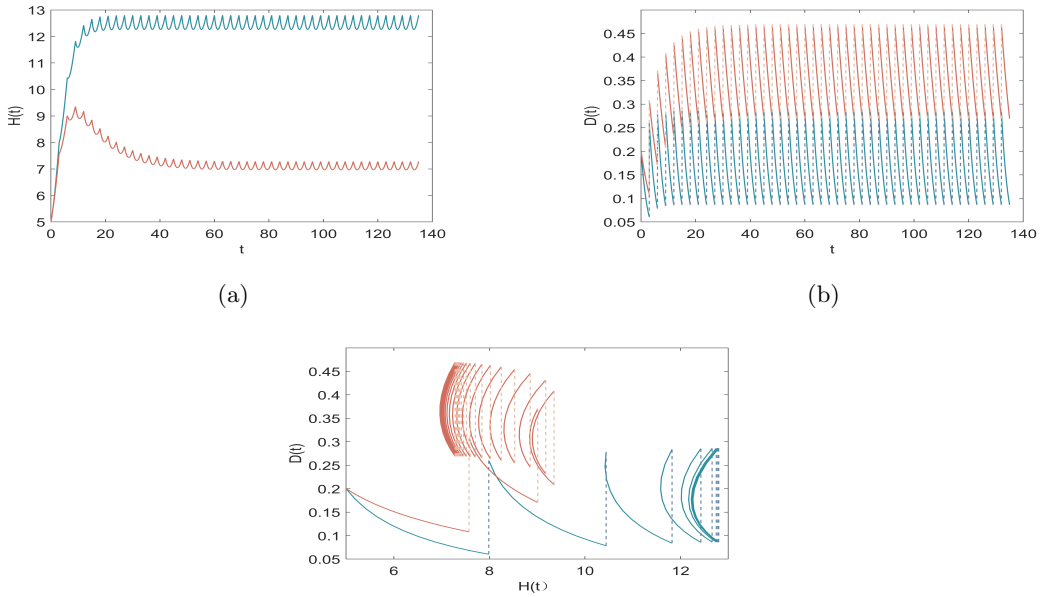

(a) (b) (c)

Figure 6. Comparison of linear and nonlinear drug elimination rates. (a) Time series of tumor cell concentration $H(t)$: Blue line (linear elimination, $D'(t) = -\beta D(t)$) shows simple decay; rad line (nonlinear elimination, Michaelis-Menten function) exhibits a two-phase effect (initial stimulation followed by inhibition). (b) Time series of drug concentration $D(t)$: Linear elimination (red) decays exponentially, while nonlinear elimination (blue) shows saturated decay. (c) Phase portrait of $H(t)$ vs. $D(t)$: Nonlinear elimination captures more complex dynamical behaviors consistent with clinical observations. Initial condition: $(H_0, D_0) = (5, 0.2)$. Other parameters are the same as that in Figure 2.

minimal influence on the system's eventual periodic behavior. In contrast to traditional models, which often assume linear drug decay (neglecting enzymatic degradation kinetics) or overlook the discrete nature of impulsive treatment schedules and sensitivity to initial conditions, our framework introduces three innovations:

(i) It couples Michaelis–Menten pharmacokinetics with discrete-time pulse chemotherapy to mimic clinical administration protocols;

(ii) it identifies the R_1 and R_2 thresholds and rigorously proves the existence of stable positive periodic solutions, providing dynamical insights absent in linear models;

(iii) it formalizes the influence of initial values and residual drug effects, two clinically critical factors often neglected in prior mathematical modeling of chemotherapy. These innovations strengthen the model's translational relevance by reflecting the biological and clinical complexity of real treatment scenarios.

The numerical simulations further clarify the biological implications of these theoretical findings. The results indicate that dose intensity and treatment interval are two dominant determinants of long-term therapeutic outcome. Within the parameter regimes considered here, increasing the impulsive dose can drive the system from tumor permanence to tumor eradication, whereas changes in the treatment interval may induce substantial transitions in long-term system behavior. Moreover, the simulations show that initial conditions can affect the asymptotic state in the bistable regime, implying that residual drug level and baseline tumor burden may influence the eventual treatment trajectory. These findings highlight that long-term treatment outcome cannot always be inferred from dose magnitude alone.

Despite its analytical rigor, the model necessarily incorporates simplifying assumptions to maintain tractability, resulting in several limitations. First, it assumes homogeneous tissue distribution, thereby neglecting spatial heterogeneity in drug penetration, tumor cell diffusion, and local enzymatic activity. This simplification avoids the complexity of partial differential equations while enabling explicit derivation of stability conditions for R_1, R_2, and fixed points. Future work will address this by incorporating "spatio-enzymatic integration," i.e., spatial diffusion terms and region-specific enzymatic activity parameters, to capture heterogeneous drug degradation and tumor spread. Second, the model employs idealized impulsive inputs, omitting interpatient variability in enzymatic degradation rates, drug absorption, and injection timing. This choice simplifies analysis and clarifies the relationships between initial values, residual drug, and the R_1/R_2 thresholds. Subsequent extensions will introduce stochastic perturbations to account for patient-specific pharmacokinetics and to model dynamic feedback between residual drug levels and treatment response. Third, the model does not yet incorporate dynamic bidirectional feedback loops between residual drug accumulation and tumor progression, focusing instead on static correlations to prove key stability and bifurcation results. A dedicated feedback module will be developed in future work to capture these interactions and further enhance biological realism.

From both theoretical and translational perspectives, the model provides several useful insights. The thresholds R_1 and R_2 offer transparent analytical criteria for distinguishing tumor eradication from permanence, while the existence of stable positive periodic solutions and bistable behavior reveals that repeated chemotherapy may generate qualitatively different long-term outcomes under different dose levels, treatment intervals, and initial conditions. Biomedically, the model suggests that treatment effectiveness depends not only on dose intensity, but also on whether the dosing interval allows residual drug exposure to remain within a therapeutically effective range. It also highlights that nonlinear elimination may alter both the duration of effective drug action and the residual concentration before the next treatment cycle, thereby influencing cumulative efficacy and potential toxicity.

These limitations point to several promising directions for future research, including the incorporation of spatial diffusion and heterogeneous enzymatic activity, stochastic perturbations and patient-specific uncertainty, toxicity-related variables, and feedback mechanisms between residual drug accumulation and tumor progression. In addition, combining the present framework with optimal control, data-driven parameter estimation, or multiscale modeling may help bridge the gap between mathematical analysis and personalized treatment design.

In summary, this study establishes a mathematically rigorous and biologically interpretable framework for analyzing impulsive chemotherapy under Michaelis–Menten nonlinear drug elimination. By prioritizing residual drug monitoring, identifying critical stability thresholds, and accounting for both pharmacokinetic complexity and impulsive treatment schedules, it provides a useful basis for understanding how repeated chemotherapy may generate distinct long-term outcomes. By identifying explicit periodic drug dynamics, deriving threshold conditions for tumor extinction and permanence, and clarifying the effects of dose, treatment interval, nonlinear elimination, and initial values, the model offers a meaningful step toward more realistic and clinically informative mathematical models of chemotherapy scheduling and tumor control.

Author contributions

Changtong Li: Writing-Original draft. Lifeng Wang: Conceptualization, Theoretical analysis. Xiaozhou Feng: Funding acquisition. Yuntao Liu: Visualization.

References

[1] I. Bashkirtseva, L. Ryashko and J. M. Seoane, *Chaotic transitions in a tumor-immune model under chemotherapy treatment*, Communications in Nonlinear Science and Numerical Simulation, 2024, 132, 107946.

[2] S. L. Beal, *Computation of the explicit solution to the Michaelis–Menten equation*, Journal of Pharmacokinetics and Biopharmaceutics, 1983, 11, 641–657.

[3] D. Belkić, *The Euler T and Lambert W functions in mechanistic radiobiological models with chemical kinetics for repair of irradiated cells*, Journal of Mathematical Chemistry, 2018, 56, 2133–2193.

[4] Y. L. Chen, M. C. Chang and W. F. Cheng, *Metronomic chemotherapy and immunotherapy in cancer treatment*, Cancer Letters, 2017, 400, 282–292.

[5] Y. S. Cho and H. S. Lim, *Comparison of various estimation methods for the parameters of Michaelis–Menten equation based on in vitro elimination kinetic simulation data*, Translational and Clinical Pharmacology, 2018, 26(1), 39–47.

[6] P. Das, S. Das and R. K. Upadhyay, *Optimal treatment strategies for delayed cancer-immune system with multiple therapeutic approach*, Chaos, Solitons & Fractals, 2020, 136, 109806.

[7] D. A. Drexler and L. Kovács, *Optimization of impulsive discrete-time tumor chemotherapy*, 2019 First International Conference on Societal Automation (SA), 2019, 1–7.

[8] M. Farhan, Z. Ling and Waseem, *A novel intelligent framework for assessing within-host transmission dynamics of Chikungunya virus using an unsupervised stochastic neural network approach*, Computational Biology and Chemistry, 2025, 117, 108380.

[9] M. Goličnik, *Explicit reformulations of the Lambert W-omega function for calculations of the solutions to one-compartment pharmacokinetic models with Michaelis–Menten elimination kinetics*, European Journal of Drug Metabolism and Pharmacokinetics, 2011, 36, 121–127.

[10] J. J. Jiao, Z. Z. Liu and L. M. Li, *Threshold dynamics of a stage-structured single population model with non-transient and transient impulsive effects*, Applied Mathematics Letters, 2019, 97, 88–92.

[11] V. A. Kuznetsov, I. A. Makalkin and M. A. Taylor, *Nonlinear dynamics of immunogenic tumors: Parameter estimation and global bifurcation analysis*, Bulletin of Mathematical Biology, 1994, 56(2), 295–321.

[12] A. Lakmeche and O. Arino, *Bifurcation of non trivial periodic solutions of impulsive differential equations arising chemotherapeutic treatment*, Nonlinear Analysis: Theory, Methods & Applications, 2000, 7, 265–287.

[13] W. M. Lau, A. W. White and S. J. Gallagher, *Scope and limitations of the co-drug approach to topical drug delivery*, Current Pharmaceutical Design, 2008, 14(8), 794–802.

[14] C. T. Li, X. Z. Feng and Y. Z. Wang, *Complex dynamics of Beddington–DeAngelis-type predator–prey model with nonlinear impulsive control*, Complexity, 2020, 2020, 8829235.

[15] C. T. Li, Y. T. Liu, and Y. Z. Wang, *Dynamic modeling of the glucose–insulin system with inhibitors impulsive control*, Mathematical Methods in the Applied Sciences, 2024, 47(15), 18745–18760.

[16] S. Li, M. Ullah and S. Ullah, *A novel stochastic neural network framework for modeling and simulation of within-host Chikungunya virus transmission with latency*, Knowledge-Based Systems, 2025, 329, 114412.

[17] S. G. Liliopoulos, G. S. Stavrakakis and K. S. Dimas, *Linear and non-linear optimal control methods to determine the best chemotherapy schedule for most effectively inhibiting tumor growth*, Biomedicines, 2025, 13(2), 13020315.

[18] B. Liu, Y. J. Zhang and L. S. Chen, *The dynamical behaviors of a Lotka–Volterra predator–prey model concerning integrated pest management*, Nonlinear Analysis: Real World Applications, 2005, 6(2), 227–243.

[19] Y. Liu, Y. H. Ma and C. H. Yang, *Modeling the nonmonotonic immune response in a tumor–immune system interaction*, Symmetry, 2024, 16(6), 676.

[20] L. Y. Pang, L. Shen and Z. Zhao. *Mathematical modelling and analysis of the tumor treatment regimens with pulsed immunotherapy and chemotherapy*, Computational and Mathematical Methods in Medicine, 2016, 2016, 6260474.

[21] L. Pierik, P. McDonald and A. R. A. Anderson, *Second-order effects of chemotherapy pharmacodynamics and pharmacokinetics on tumor regression and cachexia*, Bulletin of Mathematical Biology, 2024, 86, 72.

[22] L. G. de Pillis, W. Gu and A. E. Radunskaya, *Mixed immunotherapy and chemotherapy of tumors: Modeling, applications and biological interpretations*, Journal of Theoretical Biology, 2006, 238(4), 841–862.

[23] S. A. Saganuwan, *Application of modified Michaelis–Menten equations for determination of enzyme inducing and inhibiting drugs*, BMC Pharmacology and Toxicology, 2021, 22, 57.

[24] G. Song, G. Z. Liang and T. H. Tian, *Mathematical modeling and analysis of tumor chemotherapy*, Symmetry, 2022, 14(4), 704.

[25] H. Sung, J. Ferlay and R. L. Siegel, *Global cancer statistics 2020: GLOBOCAN estimates of incidence and mortality worldwide for 36 cancers in 185 countries*, CA A Cancer Journal for Clinicians, 2021, 71(3), 209–249.

[26] X. W. Tan, S. Y. Tang and X. Z. Chen, *A stochastic differential equation model for pest management*, Advances in Difference Equations, 2017, 2017, 197.

[27] B. Tang, Y. N. Xiao and J. H. Wu, *A piecewise model of virus-immune system with two thresholds,* Mathematical Biosciences, 2016, 278, 63–76.

[28] S. Y. Tang, S. Li and B. Tang, *Hormetic and synergistic effects of cancer treatments revealed by modelling combinations of radio- or chemotherapy with immunotherapy*, BMC Cancer, 2023, 23, 1040.

[29] S. Y. Tang and Y. N. Xiao, *One-compartment model with Michaelis–Menten elimination kinetics and therapeutic window: An analytical approach*, Journal of Pharmacokinetics and Pharmacodynamics, 2007, 34, 807–827.

[30] Z. Veitch, O. F. Khan and D. Tilley, *Impact of cumulative chemotherapy dose on survival with adjuvant FEC-D chemotherapy for breast cancer*, Journal of the National Comprehensive Cancer Network, 2019, 17(8), 957–967.

[31] Y. Wang, L. Y. Yang and L. Mao, *SGLT2 inhibition restrains thyroid cancer growth via G1/S phase transition arrest and apoptosis mediated by DNA damage response signaling pathways*, Cancer Cell International, 2022, 22, 74.

[32] Y. Z. Wang, Samreen and S. Ullah, *Numerical assessment of multiple vaccinations to mitigate the transmission of COVID-19 via a new epidemiological modeling approach*, Results in Physics, 2023, 52, 106889.

[33] J. J. Wu and D. J. Waxman, *Immunogenic chemotherapy: Dose and schedule dependence and combination with immunotherapy*, Cancer Letters, 2018, 419, 210–221.

[34] D. D. Yan, M. Q. He and S. Y. Tang, *Incorporating drug adherence stochasticity into pharmacokinetics and pharmacodynamics to understand the HIV transmission dynamics through a multiscale system*, SIAM Journal on Applied Mathematics, 2025, 85, 2566–2590.

[35] M. Yosef and S. Bunimovich-Mendrazitsky, *Mathematical model of MMC chemotherapy for non-invasive bladder cancer treatment*, Frontiers in Oncology, 2024, 14, 1352065.

[36] L. F. Zhang, H. B. Xie and Y. Q. Wang, *Pharmacodynamic parameters of pharmacokinetic/pharmacodynamic (PK/PD) integration models*, Frontiers in Veterinary Science, 2022, 9, 860472.

[37] Q. Zhao, L. Y. Pang and Q. Y. Li, *Analysis of a hybrid impulsive tumor-immune model with immunotherapy and chemotherapy*, Chaos, Solitons & Fractals, 2021, 144, 110617.

[38] Z. Zhao, X. Q. Zhang and L. S. Chen, *The effect of pulsed harvesting policy on the inshore–offshore fishery model with the impulsive diffusion*, Nonlinear Dynamics, 2011, 63, 537–545.

Received January 2026; Accepted May 2026; Available online June 2026.